Quaternary Science Reviews 224 (2019) 105971

Contents lists available at ScienceDirect

Quaternary Science Reviews

journal homepage: www.elsevier.com/locate/quascirev

1200 years of Upper Missouri River streamflow reconstructed from tree rings

Justin T. Martin [a, *], Gregory T. Pederson [a], Connie A. Woodhouse [b, c], Edward R. Cook [d], Gregory J. McCabe [e], Erika K. Wise [f], Patrick Erger [g], Larry Dolan [h], Marketa McGuire [i], Subhrendu Gangopadhyay [i], Katherine Chase [j], Jeremy S. Littell [k], Stephen T. Gray [k], Scott St. George [l], Jonathan Friedman [m], Dave Sauchyn [n], Jeannine St. Jacques [o], John King [p]

[a] U.S. Geological Survey, Northern Rocky Mountain Science Center, Bozeman, MT, USA
[b] School of Geography and Development, University of Arizona, Tucson, AZ, USA
[c] Laboratory of Tree-Ring Research, University of Arizona, Tucson, AZ, USA
[d] Lamont-Doherty Earth Observatory, Palisades, NY, USA
[e] U.S. Geological Survey, Water Resources Division, Denver, CO, USA
[f] Department of Geography, University of North Carolina, Chapel Hill, NC, USA
[g] U.S. Bureau of Reclamation, Great Plains Regional Office, Billings, MT, USA
[h] Montana Department of Natural Resources and Conservation, Helena, MT, USA
[i] U.S. Bureau of Reclamation, Technical Service Center, Denver, CO, USA
[j] U.S. Geological Survey, Wyoming-Montana Water Science Center, Helena, MT, USA
[k] U.S. Geological Survey, Alaska Climate Adaptation Science Center, Anchorage, AK, USA
[l] Department of Geography, Environment and Society, University of Minnesota, Minneapolis, MN, USA
[m] U.S. Geological Survey, Fort Collins Science Center, Ft. Collins, CO, USA
[n] Department of Geography and Environmental Studies, University of Regina, Regina, Saskatchewan, Canada
[o] Department of Geography, Planning and Environment, Concordia University, Montreal, Quebec, Canada
[p] Lone Pine Research, Bozeman, MT, USA

ARTICLE INFO

Article history:
Received 26 July 2019
Received in revised form
27 September 2019
Accepted 28 September 2019
Available online 15 October 2019

Keywords:
Holocene
Paleoclimatology
North America
Tree-rings
Streamflow
Upper Missouri River
Reconstruction

ABSTRACT

Paleohydrologic records can provide unique, long-term perspectives on streamflow variability and hydroclimate for use in water resource planning. Such long-term records can also play a key role in placing both present day events and projected future conditions into a broader context than that offered by instrumental observations. However, relative to other major river basins across the western United States, a paucity of streamflow reconstructions has to date prevented the full application of such paleohydrologic information in the Upper Missouri River Basin. Here we utilize a set of naturalized streamflow records for the Upper Missouri and an expanded network of tree-ring records to reconstruct streamflow at thirty-one gaging locations across the major headwaters of the basin. The reconstructions explain an average of 68% of the variability in the observed streamflow records and extend available records of streamflow back to 886 CE on average. Basin-wide analyses suggest unprecedented hydroclimatic variability over the region during the Medieval period, similar to that observed in the Upper Colorado River Basin, and show considerable synchrony of persistent wet-dry phasing with the Colorado River over the last 1200 years. Streamflow estimates in individual sub-basins of the Upper Missouri demonstrate increased spatial variability in discharge during the Little Ice Age (~1400–1850 CE) compared with the Medieval Climate Anomaly (~800–1400 CE). The network of streamflow reconstructions presented here fills a major geographical void in paleohydrologic understanding and now allows for a long-term assessment of hydrological variability over the majority of the western U.S.

Published by Elsevier Ltd.

* Corresponding author.
E-mail address: justinmartin@usgs.gov (J.T. Martin).

https://doi.org/10.1016/j.quascirev.2019.105971
0277-3791/Published by Elsevier Ltd.

1. Introduction

Variability in natural (i.e. unmanaged) streamflow over time reflects the complex interplay of climatic influences such as precipitation and temperature superposed on local attributes including topography, soils, geologic characteristics, and land cover, all of which affect basin hydrology (Lettenmaier and Gan, 1990; McCabe and Wolock, 2011a). Natural streamflow variability is a primary determinant of the amount of surface water available for both societal use and ecological function (Hamlet and Lettenmaier, 1999; Stewart et al., 2005). Because of the substantial influence of natural streamflow variability on water supplies, there has been considerable effort directed towards investigating both the climatic drivers and management implications of hydrologic variability, particularly in the semi-arid to arid American West (Gangopadhyay et al., 2019; Garrick et al., 2008; Lehner et al., 2017; McCabe and Wolock, 2011b; Meko et al., 2007; Woodhouse et al., 2010; Yoon et al., 2015). Observational records in the western U.S. generally span less than 100 years, and are typically inadequate for fully characterizing long-term hydrologic variability including events such as severe and sustained droughts (Woodhouse et al., 2017).

In some cases, the limitations imposed by relatively short instrumental streamflow observations can be overcome by extending those records further back in time through the generation of tree-ring based reconstructions of streamflow (Earle and Fritts, 1986; Littell et al., 2016; Meko et al., 2007; Stockton and Jacoby, 1976; Wise, 2010a; Woodhouse, 2001). Historically, most streamflow reconstructions have been focused on basins such as the Upper Colorado River Basin (UCRB) (Hidalgo et al., 2000; Meko et al., 2007; Stockton and Jacoby, 1976; Woodhouse et al., 2006) where surface water is derived primarily from winter precipitation originating in the Pacific Ocean that is subsequently delivered to mid- to high-elevations as snowfall each year (Christensen and Lettenmaier, 2006).

Situated to the north and east of the UCRB are the mountain headwaters of the Missouri River, the longest river in North America draining the largest independent river basin in the United States. For the purpose of this study, the Upper Missouri River Basin (UMRB) is defined as the part of the Missouri basin from roughly 105° W longitude to the continental divide, and north to south from the Milk River in Canada to the South Platte River in Colorado (Fig. 1). In contrast to the UCRB, long-term hydrologic variability across the UMRB remains mostly uncharacterized (Ho et al., 2016). With the exception of streamflow reconstructions for several sites in the Yellowstone and Platte basins (Graumlich et al., 2003; Watson et al., 2009; Woodhouse, 2001), no systematic effort aimed at generating a network of long reconstructions of natural streamflow in the UMRB has been successfully undertaken prior to now.

Using long-term records of UMRB streamflow, we hope to improve understanding of the potential spatial extent and persistence of high and low streamflow events across the greater U.S. Rocky Mountain region. Synchronous periods of drought in both the UMRB and UCRB during the 1930s, 1950s, late 1980s, and early 2000s suggest that extended hydrologic drought tends to be widespread over much of the northern and southern Rockies. However, this observation runs somewhat counter to evidence that anomalies in both precipitation and snowpack development exhibit a north-south dipole pattern across much of the western U.S. (Dettinger et al., 1998; Pederson et al., 2011; Wise, 2010b). Specifically, observations suggest that northern regions (above ~40° latitude) tend to be anomalously dry when the southern regions are anomalously wet and vice-versa over timescales ranging from inter-annual to multi-decadal (Dettinger et al., 1998; Pederson et al., 2011).

Large-scale oceanic/atmospheric teleconnections such as the Atlantic Multi-decadal Oscillation (AMO), Pacific Decadal Oscillation (PDO), and El Niño-Southern Oscillation (ENSO) exhibit significant control over dominant storm tracks, precipitation, and resulting streamflow patterns across the western U.S. (Enfield et al., 2001; Hidalgo and Dracup, 2003; McCabe et al., 2004; Redmond and Koch, 1991). Our understanding of the long-term influence of multidecadal-scale climate variability on streamflow across the western U.S. is again relatively limited since most gage-based estimates of natural streamflow in the western U.S. often only capture one to three full cycles of these important decadal to multi-decadal climate drivers. A multi-century comparison of the AMO and UCRB streamflow since the 1500s suggests that Atlantic sea-surface temperatures have exhibited significant low-frequency control over Colorado river flows when filtered to emphasize the 64–80 year signal in the reconstructed Lee's Ferry record (Nowak et al., 2012). Additionally, a strong 60 year periodicity evident in 820 years of reconstructed precipitation over the Yellowstone plateau indicates that a primary driver of streamflow in the UMRB operates on a similarly low-frequency cycle (Gray et al., 2007). Similar assessments have not been made across the UMRB due to the lack of a network of extended streamflow records, making unclear the potential spatial and temporal influence of these low-frequency climate dynamics on UMRB streamflow and the degree to which they are synchronized with the UCRB.

Paleohydrologic records in the western U.S. also help provide a multi-century context for severe and persistent wet and dry conditions. For example, the drought that persisted over the UCRB (Prairie et al., 2008; Udall and Overpeck, 2017; Woodhouse et al., 2010) through the early 2000s was unprecedented over the observational period. Reconstructions of UCRB streamflow suggest that such drought conditions are rare, but have likely occurred in the past (Meko et al., 2007). In fact, in the UCRB, even more sustained periods of drought occurred during the mid 1100s (Woodhouse et al., 2010). However, in the UMRB, we have lacked the extended records necessary to understand recent droughts from a long-term perspective.

Finally, recent evidence suggests that significant hydroclimatic changes have occurred across the UMRB in recent decades including a consistent decrease in annual streamflow from the mountain headwater regions (Norton et al., 2014), an increasing trend in March–July temperatures (Wise et al., 2018), reductions in annual snow-to-rain ratios (Wise et al., 2018), increasingly extreme precipitation events (Livneh et al., 2016), and higher flood frequencies (Livneh et al., 2016). Changes such as more extreme precipitation events as well as resulting flood events (Livneh et al., 2016) are consistent with the projected impacts of warming temperatures on precipitation variability (Pendergrass et al., 2017), including areas such as the UMRB. However, in the absence of long-term hydrologic records for the region, it is uncertain if these changes represent a shift to new conditions associated with warmer temperatures in the UMRB or simply a return to previous conditions not represented in the short observational record.

Uncertainties in the understanding of long-term streamflow variability in the UMRB, the effects of these uncertainties on water resource management and planning in the basin, and the influence on how we contextualize changing hydro-climatic conditions, highlight a pressing need for extended streamflow estimates for the region. In recognition of this need, we draw on a newly compiled set of naturalized streamflow records for the UMRB and an expanded collection of tree-ring records from the region to explore the following questions: **1)** Is it possible to skillfully reconstruct streamflow records in the UMRB? **2)** What do long-term records reveal about the temporal and spatial characteristics of basin-wide streamflow variability in the UMRB such as the persistence of dry

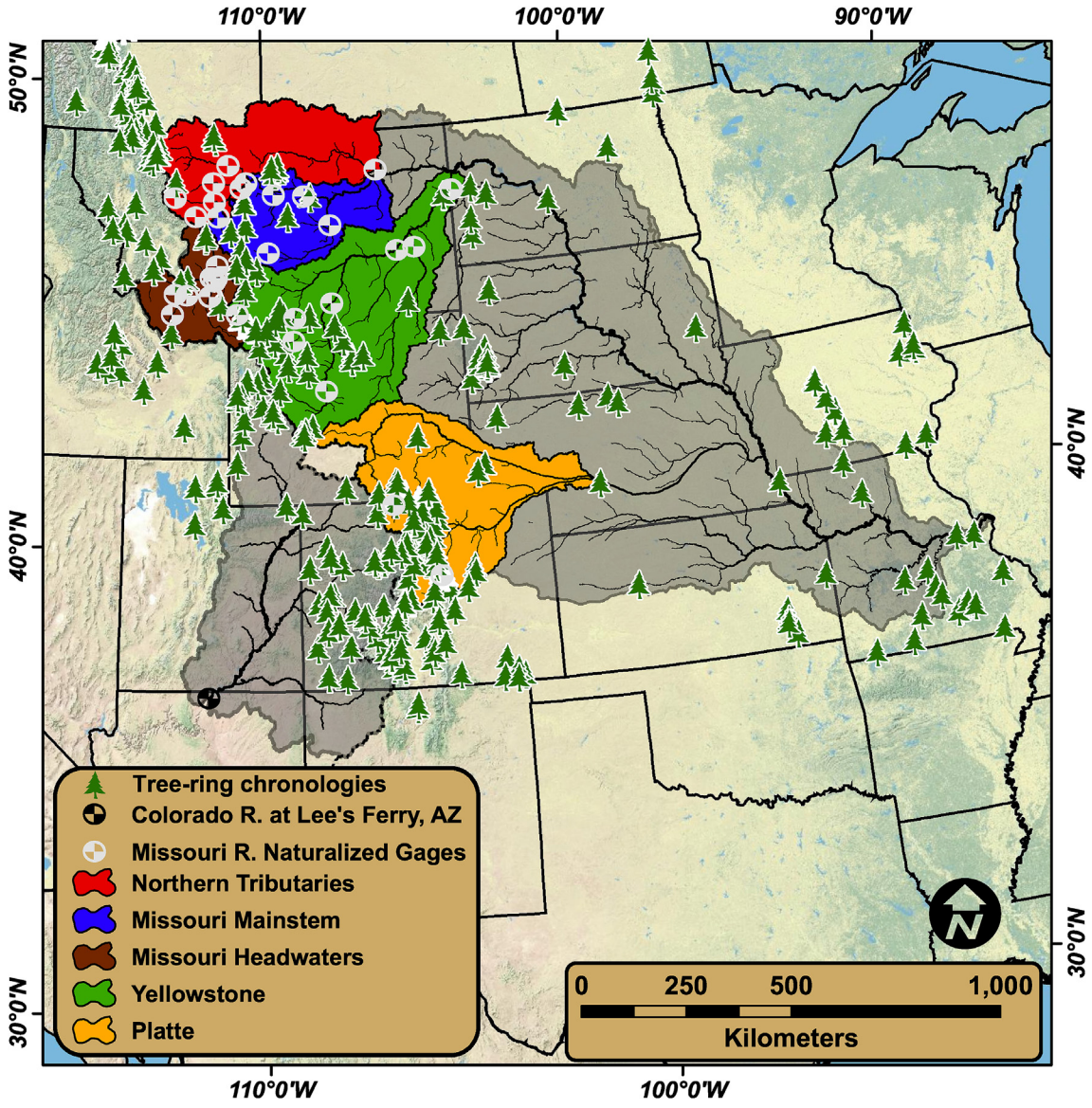

Fig. 1. The 31 reconstructed naturalized Upper Missouri River Basin stream gages, and 374 potential predictor chronologies from 22 different species of trees falling within 250 km of the basin. The Upper Missouri River Basin (UMRB) is shown in color. Its major sub-basins identified through cluster analysis of gage records are also shown. The Upper Colorado River Basin (UCRB) to the south and west, and its major outflow gage at Lee's Ferry AZ are shown for reference. (For interpretation of the references to color in this figure legend, the reader is referred to the Web version of this article.)

and wet periods and the timing of severe drought in the past? **3)** How do these events compare with droughts and pluvials in the UCRB over past centuries?

2. Methods and data

2.1. Naturalized streamflow data

An initial collection of over 300 raw-gaged, and naturalized streamflow records were compiled from 252 gaging locations within Missouri River Hydrologic Region 10 (Seaber et al., 1987) and were subsequently screened to produce a set including only the naturalized flow records, or records deemed to reasonably represent natural flow with limited modifications from human activity (Falcone, 2011; Slack et al., 1994). The final network of streamflow records for the instrumental period used in generating the paleohydrologic reconstructions contains a total of 31 streamflow records spanning roughly the 1930s through 2010 CE (Brekke et al., 2010; Cary and Parrett, 1996; Chase, 2014; Gangopadhyay and Pruitt, 2010; Slack et al., 1994) (Fig. 1, Table 1). To reduce the complexity of the gage network we performed a hierarchical cluster analysis (clustering based on Ward's method) (Murtagh, 1985) of the 31 naturalized streamflow records over the 40 years common to all gages (1950–1989). Stream gages clustered neatly into groups reflecting their geographic proximity or location above/below other gages on the same river (Fig. 1). Cluster membership for specific gages then was used for dimension reduction in several analyses described below.

2.2. Tree-ring data

A network of climate sensitive tree-ring data exists for the Missouri River basin and surrounding regions that have previously been used to reconstruct snowpack, the summer Palmer Drought

Table 1
Location and authors of the 31 naturalized streamflow gage records reconstructed across the Upper Missouri River Basin. Bold text denotes gages used in the Upper Missouri River Basin composite streamflow reconstruction.

	USGS number	River	Gage Name	Latitude	Longitude	Authors
1	6016000	Beaverhead	Barretts	45.12	−112.75	Cary, Parrett
2	**6025500**	**Big Hole**	**Melrose**	**45.53**	**−112.7**	**Erger, Devore, Brekke**
3	6287000	Bighorn	St. Xavier	45.32	−107.92	Phillips, Aycock
4	**6207500**	**Clarks Fork Yellowstone**	**Belfry**	**45.01**	**−109.07**	**HCDN**
5	6073500	Dearborn	Craig	47.2	−112.1	Dolan
6	6052500	Gallatin	Logan	45.89	−111.44	Erger, Devore, Brekke
7	6036650	Jefferson	Three Forks	45.9	−111.6	Cary, Parrett
8	6114700	Judith	Winifred	47.67	−109.65	Cary, Parrett
9	**6041000**	**Madison**	**McAllister**	**45.49**	**−111.63**	**Cary, Parrett**
10	**6042500**	**Madison**	**Three Forks**	**45.82**	**−111.5**	**Erger, Devore, Brekke**
11	**6101500**	**Marias**	**Chester**	**48.31**	**−111.08**	**Cary, Parrett**
12	6174500	Milk	Nashua	48.13	−106.36	Gangopadhyay
13	**6090800**	**Missouri**	**Ft. Benton**	**47.82**	**−110.67**	**Cary, Parrett**
14	**6115200**	**Missouri**	**Landusky**	**47.63**	**−108.69**	**Cary, Parrett**
15	**6054500**	**Missouri**	**Toston**	**46.15**	**−111.42**	**Erger, Devore, Brekke**
16	**6120500**	**Musselshell**	**Harlowton**	**46.43**	**−109.84**	**Cary, Parrett**
17	**6130500**	**Musselshell**	**Mosby**	**46.99**	**−107.89**	**Dolan**
18	**6620000**	**North Platte**	**North Gate**	**40.94**	**−106.34**	**HCDN**
19	**6326500**	**Powder**	**Locate**	**46.43**	**−105.31**	**Chase**
20	6023000	Ruby	Twin Bridges	45.51	−112.33	Erger, Devore, Brekke
21	6282000	Shoshone	Buffalo Bill	44.52	−109.1	Phillips, Aycock
22	**6077500**	**Smith**	**Eden**	**47.19**	**−111.39**	**Cary, Parrett**
23	**6707500**	**South Platte**	**South Platte**	**39.41**	**−105.17**	**Denver Water**
24	6079500	Sun	Gibson Res	47.6	−112.76	Cary, Parrett
25	**6089000**	**Sun**	**Vaughn**	**47.53**	**−111.51**	**Cary, Parrett**
26	**6108000**	**Teton**	**Dutton**	**47.93**	**−111.55**	**Cary, Parrett**
27	6108800	Teton	Loma	47.93	−110.51	Cary, Parrett
28	**6308500**	**Tongue**	**Miles City**	**46.38**	**−105.85**	**Chase**
29	6259000	Wind	Boysen	43.42	−108.18	Phillips, Aycock
30	6191500	Yellowstone	Corwin Springs	45.11	−110.79	Chase
31	**6329500**	**Yellowstone**	**Sidney**	**47.68**	**−104.16**	**Chase**

Severity Index, and streamflow in other basins (Fig. 1), (Cook et al., 2004; Pederson et al., 2011; Wise, 2010a; Woodhouse et al., 2006). The network contains trees with a diversity of seasonal hydroclimatic sensitivities that are typically related to tree species, elevation, and topographic setting (St. George, 2014; Wettstein et al., 2011). The diversity of climate-growth responses makes this network of tree-ring chronologies suitable for reconstructing streamflow for a network of gages located in a basin that exhibits complex climate and streamflow responses due to a range of factors related to geography, soils, and climate dynamics (Wise et al., 2018). For inclusion in the reconstruction process, all tree-ring records were required to extend prior to the year 1800 CE, which resulted in a final dataset of 374 chronologies, 107 of which are new, updated, or were not previously publicly available prior to this research effort. The full set of individual raw ring-width records are now available on the International Tree-Ring Data Bank (ITRDB) hosted by the National Oceanic and Atmospheric Administration (NOAA) National Climatic and Data Center (NCDC) at https://www.ncdc.noaa.gov/paleo-search/study/26831.

Tree-ring chronologies were constructed from these raw ring-width records by first removing the non-climatic biological growth curve from the individual records (i.e. a process known as "detrending") following methods Melvin and Briffa (2008). Removal of geometric tree-growth artifacts and the production of the standardized ring-width indices was performed using standard methods (Cook et al., 2016). Specifically, here we used an age-dependent spline of unconstrained slope with initial stiffness set to 20-years (Melvin et al., 2007). This individual-series detrending method preserves low-frequency climate signals in a similar fashion to detrending with a negative exponential curve, but with some advantages over the juvenile growth years. However, the unconstrained slope of the detrending spline will remove positive monotonic growth trends if present. The final ring-width index (RWI) chronologies were therefore constructed by calculating a bi-weight robust mean from the power-transformed residuals of the individually detrended ring-width series, reducing the potential for trend distortion from end effects that can result from the ratio method of chronology calculation. Variance stabilization was performed using the Rbar method with correction of trend in variance provided by an age-dependent spline. The length of all chronologies was truncated when the number of individual ring-width measurement series in the chronology fell below five.

2.3. Climate data

The climate data used were the 4-km (km) by 4-km gridded monthly temperature and precipitation data from the **P**recipitation-elevation **R**egression on **I**ndependent **S**lopes **M**odel (PRISM) dataset (Daly et al., 2008) for water years (October–September) 1900 through 2014 CE. The gridded monthly temperature and precipitation data were used as inputs to a monthly time-step water balance model (MWBM) from McCabe and Wolock (2011b) to generate additional hydrologic variables related to streamflow. All hydroclimatic variables then were aggregated to U.S. Geological Survey 8-digit hydrologic units (HU) (Seaber et al., 1987) for the UMRB. Water balance model parameters used for this study were taken from parameter sets developed in previous studies (McCabe and Wolock, 2011a; Wise et al., 2018), and soil-moisture-storage capacity for each HU was computed using the available water-capacity values from the State Soil Geographic Data Base (STATSGO) dataset by assuming a 1-m rooting depth, U.S. Department of Agriculture (1994). Additional details regarding the water balance model and evaluation of the model are described in McCabe and Wolock (2011b). See E.K. Wise et al. (2018) for further information on the verification of input climate data, and additional details on model performance over the Missouri River

Basin.

2.4. Climate informed reconstruction model development

Streamflow is controlled by a diversity of season-specific climate factors that vary by sub-basin (e.g. precipitation, temperature, snow accumulation and melt) (Dettinger et al., 2004; Hamlet and Lettenmaier, 1999; Lettenmaier and Gan, 1990; Wise et al., 2018). Likewise, in the UMRB the dominant long-lived tree species span a gradient of moisture to energy limitations (St. George, 2014; Wettstein et al., 2011), and often exhibit different dominant seasonal growth responses to moisture availability, none of which perfectly reflect the seasonal controls on streamflow. Due to both the complexity of climate-growth responses of the tree species within and surrounding the UMRB and sub-basin level responses of streamflow to climate (Wise et al., 2018), reconstructing streamflow for a network of gages across the basin therefore requires novel approaches to using tree-ring records as proxies for discharge. Accordingly, here we develop a "climate-informed" methodology for reconstructing streamflow in the UMRB that seeks to match the dominant climate drivers of annual water-year (prior Oct.1 to Sept. 30) streamflow at each gage to the differing climate-growth responses by optimally integrating this information into a regression modeling and reconstruction framework.

In this "climate-informed" modeling approach, we screened all tree-ring chronologies for sensitivity to any of nine climate variables known to influence seasonal streamflow: precipitation, temperature, actual evapotranspiration, potential evapotranspiration, soil moisture, annual water balance (precipitation minus potential evapotranspiration), growing season moisture deficit (potential evapotranspiration minus actual evapotranspiration), and cool season accumulated snowpack using observed April 1 snow water equivalent (SWE) (original Natural Resource Conservation Service data compiled and presented within Wise et al., 2018), and MWBM April 1 SWE. Any chronology that was not significantly correlated (at a 95 percent confidence level ($p \leq 0.05$)) to a particular climate variable was removed from the potential predictor pool associated with that specific climate variable. This approach allowed us to produce subsets of predictor chronologies significantly correlated with each climate variable and arranged by correlation strength.

In developing regression models for reconstructing streamflow, we first transformed all streamflow records to be approximately normally distributed using a maximum likelihood estimated power transformation (Box and Cox, 1964) and then used a best-subsets approach to model selection using the "*regsubsets*" function in R package "leaps" (Lumley and Miller, 2004). The function performed an exhaustive search of a pool of potential predictor chronologies and aided in selection of the best model of each possible number of predictors. The potential predictor pool consisted of a set of up to 45 (computational limit) chronologies representing the most climatically sensitive records with respect to each of the 9 climate variables tested in the screening process. This helped to ensure that the set of tree-ring predictors resulting from the model selection for each model contained a diversity of climate signals important for streamflow. However, a maximally diverse set of predictors could not be explicitly constrained in the models because progressively longer models relied on fewer chronologies and thus, a narrower range of available tree-ring information. To guide the selection of a skillful and parsimonious model, the Mallows' Cp statistic (Mallows, 1973) was used to identify the model with the lowest difference between the statistic and parameter number. Then, selection between models with similar number of predictors was informed by identifying the model with the highest adjusted coefficient of determination (R^2). In selecting the final model, both metrics (i.e. the Cp and R^2) were weighed evenly, which balanced the potential for over fitting the model with the increased predictive power of multiple predictors.

Once the model was selected, we fit the generic model: $\mu\{streamflow \mid RWI\} = \beta_0 + \beta_1\, chronology_1 + \beta_2\, chronology_2 + \ldots + \beta_n\, chronology_n + \varepsilon$, to the transformed streamflow data, and back-transformed the predicted values. Ninety percent confidence bounds were estimated using the delta method (Dorfman, 1938) and back transformed in the same way. To extend the length of the streamflow reconstructions we then nested successive "best" fit models forward and backward in time. This was done by successively dropping any chronologies from the predictor pool that did not extend as far back in time as the predicted values of the previous fitted model. These chronologies then were replaced by the next best-correlated chronology in each of the climate screened chronology lists that had sufficient length to extend the next model either forward or backward in time. This procedure of nesting successively longer reconstructions by fitting the best model and then removing any reconstruction length-limiting chronologies was repeated until no chronologies remained in the potential predictor pool.

Because a regression reconstruction inherently underestimates the variability of the past due to a certain amount of unexplained variance in each regression model, we adapted the standard approach (Lutz et al., 2012) to restoring variance in a nested reconstruction by scaling the mean and variance of each progressively longer and less skillful model to match that of the best model over the period common to the two. We then similarly scaled the fully nested reconstruction to the target streamflow record over the calibration period of the best model. This approach maximized the length of record over which variance loss in progressively weaker models could be assessed and scaled the full nested reconstruction to the target record using the estimates of the best reconstruction model.

All streamflow reconstructions were developed in units of CFS (cubic feet per second). However, any further analyses and figures presented here were based on streamflow anomalies relative to the mean of the naturalized streamflow record from 1930 to 2010, or the z-scores of the full reconstruction.

2.5. Cross-validation of modeled streamflow

For each nested model used to reconstruct each gage record, we performed cross validation of model performance using both a leave-one-out and split-sample approach with a calibration period consisting of the earlier half of the available observed record and a verification period consisting of the latter half for the split sample method. We first generated full estimates of verification period streamflow from the model fitting process such that each annual value of observed streamflow was not included in the training data used to predict streamflow for that year. Then, based on the leave-one-out approach and using each nested model in each reconstruction, we calculated the R^2 for the observed record explained by the model parameterized only on training data (VRSQ) and did the same for the predictions made using all observed data in the calibration of the model (CRSQ). Following standard methods, and based on the split-sample calibration and verification approach, we also calculated the reduction of error statistic (RE) (Fritts, 1976) and the coefficient of efficiency (CE) (Briffa et al., 1988) for each nested model in each reconstruction.

2.6. Developing a composite record of basin-wide streamflow from individual reconstructions

To estimate the average basin-wide streamflow history from the

individual reconstructions in the network, we reduced the full network to only those gages for which the naturalized records covered the period of 1930–2010 CE (n = 17, Table 1 – bold text). This ensured that observational data used to calibrate the reconstruction models at these gages included the driest years of the 1930s Dust Bowl drought and the early 2000s. We first averaged the *z*-scores of the time series of all reconstructions within each regional cluster to define a cluster-average reconstruction. We then averaged these five reconstructions to define the basin-wide composite reconstruction. We report the 90% confidence interval for each year of the basin-wide composite as the simple average of the 90% confidence intervals of the constituent reconstructions. Likewise, the time-varying reconstruction statistics for the nested UMRB composite are reported as the simple average of the statistics for the 17 underlying reconstructions over time. This approach does underestimate the true skill in reconstructing basin-wide average flow. For example, the squared correlation between observed and modeled composite flow is 0.91 but the average VRSQ of the constituent reconstructions over the same period = 0.69. However, it provides more information about the uncertainty in the underlying records.

2.7. Spatial and temporal relationships in streamflow, and notable drought events across the UMRB and the UCRB

We explored the long-term spatial variability of streamflow both within the UMRB and across the UMRB-UCRB domain by comparing the correlation between the annual streamflow reconstruction for the most substantial gaging location in each of the five UMRB sub-basins (hereafter "main gage") as well as the reconstruction for the Colorado river at Lee's Ferry AZ (Meko et al., 2007). We examined the low-frequency coherence among these six gage records by fitting 20- and 60-year cubic smoothing splines (Cook and Kairiukstis, 1990) to the annual streamflow reconstructions, then identified the most severe drought periods as the lowest points in the splines.

We assessed temporal variability in basin-wide UMRB and UCRB streamflow by examining the agreement of wet and dry phases between the UMRB composite record and the Lee's Ferry reconstruction (Meko et al., 2007). This comparison focused on multi-decadal and longer temporal variability by using a 60-year spline of annual streamflow anomalies with the agreement across the two basins reported as the percentage of years in which the sign of the anomaly is the same.

To describe the dominant modes of quasi-periodic variability within and between streamflow records in the UMRB and UCRB, we analyzed the full common period of the reconstructions spanning 800 to 1998 CE by running a bootstrapped multi-taper method (MTM) spectral and spectral coherency analysis (Mann and Lees, 1996), on the UMRB composite and Lee's Ferry reconstructions, as well as the five UMRB sub-basins. We also assessed the strength and stationarity of the dominant modes of streamflow variability between basins using a wavelet analysis (Torrence and Compo, 1998) run on the UMRB composite record and the reconstruction for Lee's Ferry. For all analyses described in section 2.7, *z*-scores of the full reconstructed streamflow records from 800 to 1998 were used.

3. Results

3.1. Reconstruction modeling results

Of the 31 reconstructions attempted, it was possible in all cases to skillfully reconstruct natural streamflow with an average verification R^2 (VRSQ) of 0.68. The Bighorn, Madison, Jefferson, Tongue, Dearborn, Judith, Musselshell, mainstem Missouri, as well as the North and South Platte river reconstructions were particularly skillful, (VRSQ > 0.70 for the fifteen gages). Reconstruction models also performed well on the terminal mainstem gages of the Upper Missouri and Yellowstone rivers with VRSQ = 0.74 and 0.64 for the Missouri near Landusky and the Yellowstone near Sidney respectively. Several smaller rivers in the eastern portion of the basin such as the Clarks Fork of the Yellowstone and Powder, as well as several of the smaller Missouri tributaries in the northern part of the basin such as the Sun and Teton, proved most difficult to reconstruct. However, all reconstructions retained some level of skill over at least the last 700 years, maintaining a correlation with their targets >0.5 throughout the length of each nested and variance scaled reconstruction as discussed by McCarroll et al. (2015). The reconstructions extended the skillful estimates of streamflow to 886 CE on average. Streamflow reconstructions for the main gage in each of the 5 UMRB sub-regions are shown in Fig. 2 and cross-validation reconstruction statistics for each gage reconstruction in the UMRB network are shown in Table 2.

The full UMRB composite record (Fig. 3a) accurately captures the inter-annual variation in average observed streamflow anomalies (Fig. 3b) across the UMRB, with the composite record tracking the observed streamflow average with an $R^2 = 0.91$. The average reconstruction statistics for the 17 individual gage reconstructions in the composite record are shown in Fig. 4. Using these statistics for the underlying reconstructions as a basis for assessing skill in the basin-wide reconstruction, this composite record skillfully extends estimates of average basin-wide annual streamflow anomalies to 800 CE.

3.2. Spatial relationships within UMRB sub-basin flow and with UCRB streamflow

Relationships between both observed and reconstructed streamflow in the five UMRB sub-basins and the UCRB at Lee's Ferry most directly reflect the proximity of one basin to another with pairs of basins close to one another displaying the highest correlations (Figs. 1 and 5). Over the common period of 1930–1998 CE, the general spatial pattern of inter-basin correlations in the network of reconstructions (Fig. 5b) is similar to that of the observed records (Fig. 5a). In several cases, the strength of the correlations is enhanced in the reconstructions (e.g., the dipole between the northern-most gage and the UCRB), but for the most part, the correlations in the reconstructions are similar to those in the observations.

Negative relationships between long-term streamflow variability exist when comparing the basins most distantly situated from each other latitudinally. For example, the UCRB is anti-correlated with the Northern Tributaries region, indicating that the most northern region of the UMRB tends toward dryer conditions when the UCRB tends toward wetter conditions and vice versa.

Spatial patterns in the timing of the most severe droughts are also evident from the long-term records (Fig. 2). The lowest point in the 60-year spline of annual streamflow indicates a long (multi-decadal to sub-centennial) and relatively sustained period of negative flow anomalies. In the Yellowstone river this point occurs in the mid to late 1100s, closely matching the timing of the most sustained drought period observed in the UCRB (Meko et al., 2007). In the Yellowstone region, this period also marks the lowest point in the 20-year spline of streamflow indicating that the driest years of this sustained drought period were characterized by the deepest decadal to multi-decadal departure from average flow conditions. In the Northern Tributaries and Missouri Headwaters regions, the 60-year splines are lowest in the mid 1250s, again highlighting a

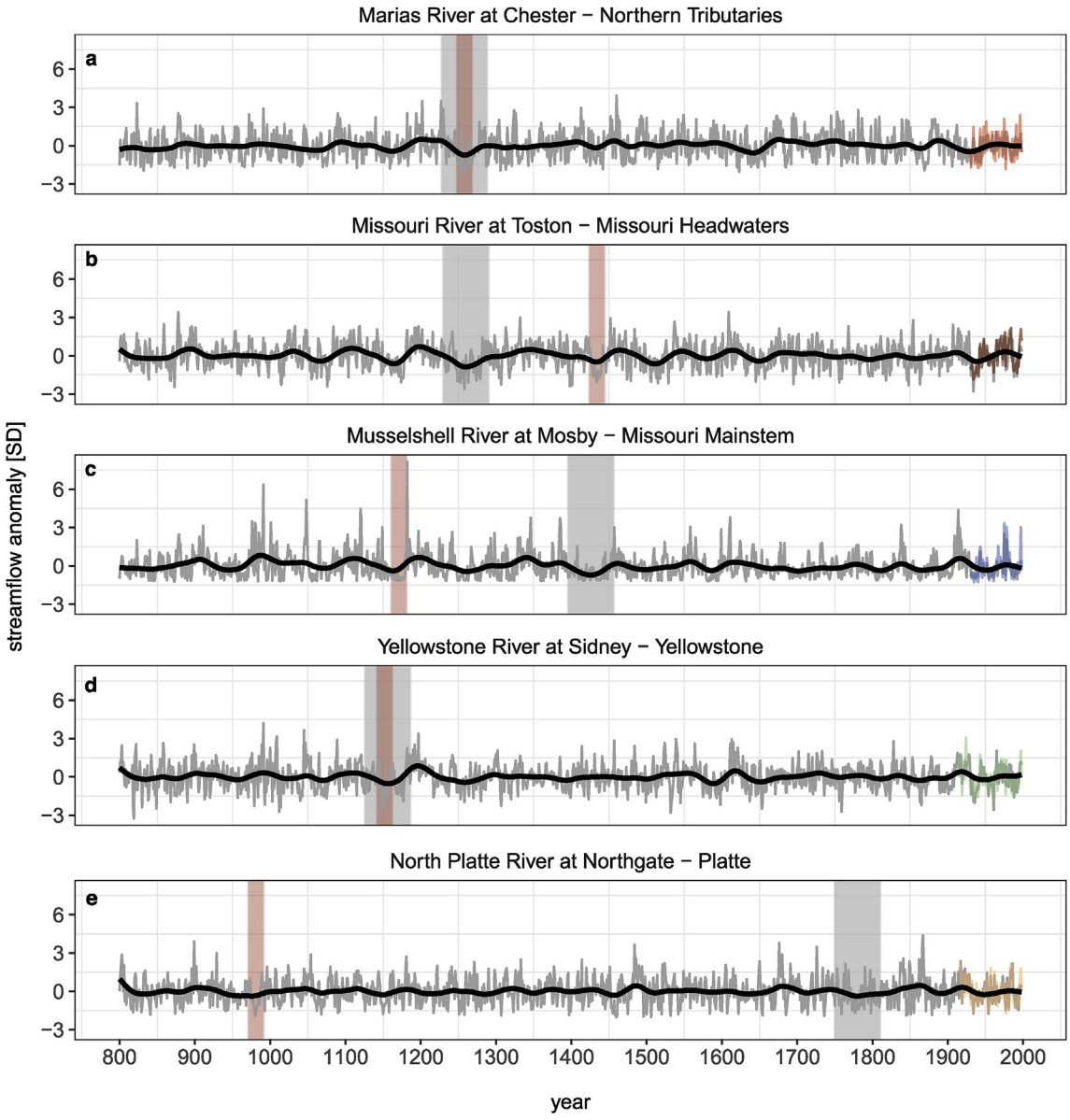

Fig. 2. Streamflow reconstructions for the most substantial gaging location in each of the 5 sub-basins. Gray lines indicate reconstructed annual values, colored lines show instrumental values overlaid on the reconstructions. Series are smoothed with a 60-year spline (heavy black line). Vertical gray bars denote 60-year periods centered on the lowest point in a 60-year spline. Red bars denote 20-year periods centered on the lowest point in a 20-year spline. (For interpretation of the references to color in this figure legend, the reader is referred to the Web version of this article.)

long-lasting departure from average flows. In the Northern Tributaries, this period was further punctuated by a severe drought period of shorter duration indicated by the lowest point in the 20-year spline. The deepest sub-centennial length drought period in the Missouri Mainstem region (and deepest bi-decadal scale drought in the Headwaters) reached its maximum depth in 1427 CE, centering a period of sustained drought across all three of the uppermost sub-regions of the basin. However, in the Platte this period is centered on the year 1780 CE, closely mirroring the timing of less-severe drought conditions in the neighboring UCRB. The most severe decadal to bi-decadal drought period in the Platte region appears in the late 900s as evidenced by a sharp decline in discharge not evident in other basins.

On a basin-wide scale, the most severe drought period in the UMRB was likely centered on the 1250s, where the 60-year spline of the composite streamflow record reaches its lowest point in the entire record. (Fig. 6a). In terms of sustained low-flow conditions, this 13th century "megadrought", reported as the second most widespread period of aridity in the American West over the last 1200 years (Cook et al., 2010), was likely unrivaled over the same time period in the UMRB, with nearly all sub-basins experiencing synchronous and sustained negative departures from average flow conditions (Fig. 6a). However, it also is likely that the depth of drought during the driest years of this multi-decadal event was nearly surpassed by the comparatively brief, but severe Dustbowl drought period of the 1930s, a period during which the 20-year spline of basin-wide flow reached its second lowest level in 1200 years (Fig. 3a).

3.3. Temporal characteristics of long-term basin-wide streamflow variability in the UMRB and the UCRB

On a basin-wide scale, streamflow in the UMRB and UCRB are moderately well correlated on an inter-annual basis. Naturalized

Table 2
Location, calibration coefficient of determination (R^2) (CRSQ), verification R^2 (VRSQ), prediction error (PE) in units of cubic feet per second (CFS), reduction of error statistic (RE), coefficient of efficiency (CE), and start year for the streamflow reconstructions produced for the UMRB. Start year denotes earliest year for which CRSQ >0.25. VRSQ was calculated using a leave-one-out approach while RE and CE were calculated using a split sample approach.

	Gage	VRSQ	CRSQ	PE [cfs]	RE	CE	Start Year
1	6287000	0.85	0.89	679.2	0.85	0.85	722
2	6041000	0.83	0.87	239.75	0.9	0.79	680
3	6259000	0.81	0.87	360.48	0.68	0.66	722
4	6620000	0.8	0.82	122.31	0.79	0.79	379
5	6042500	0.78	0.84	260.73	0.84	0.54	769
6	6036650	0.76	0.81	523.53	0.75	0.69	769
7	6308500	0.75	0.79	136.29	0.82	0.81	989
8	6115200	0.74	0.8	1957.67	0.81	0.7	769
9	6114700	0.74	0.8	58.39	0.82	0.78	818
10	6120500	0.73	0.8	78.64	0.75	0.65	1062
11	6282000	0.73	0.79	204.17	0.74	0.73	680
12	6054500	0.73	0.78	968.58	0.8	0.68	680
13	6073500	0.73	0.8	61.92	0.59	0.55	1044
14	6707500	0.73	0.78	123.14	0.75	0.75	379
15	6090800	0.7	0.75	1541.07	0.71	0.71	769
16	6077500	0.7	0.78	111.62	0.74	0.52	1027
17	6191500	0.68	0.74	489.99	0.67	0.66	882
18	6052500	0.68	0.71	208.59	0.69	0.38	680
19	6101500	0.65	0.75	268.43	0.59	0.58	1125
20	6025500	0.65	0.7	289.02	0.62	0.61	882
21	6130500	0.65	0.58	163.55	0.67	0.6	1027
22	6329500	0.64	0.69	2383.92	0.76	0.75	882
23	6089000	0.63	0.72	233.74	0.46	0.45	882
24	6108800	0.59	0.65	68.83	0.63	0.57	1154
25	6023000	0.59	0.72	63.27	0.79	0.68	1027
26	6079500	0.58	0.66	216.95	0.56	0.55	1125
27	6108000	0.56	0.72	57.42	0.5	0.41	1154
28	6326500	0.55	0.61	195.92	0.63	0.62	1260
29	6207500	0.53	0.59	160.35	0.65	0.64	769
30	6016000	0.5	0.62	112.05	0.46	0.45	1260
31	6174500	0.49	0.65	303.5	0.18	0.18	1104
32	Average	0.68	0.75	407.84	0.68	0.62	886

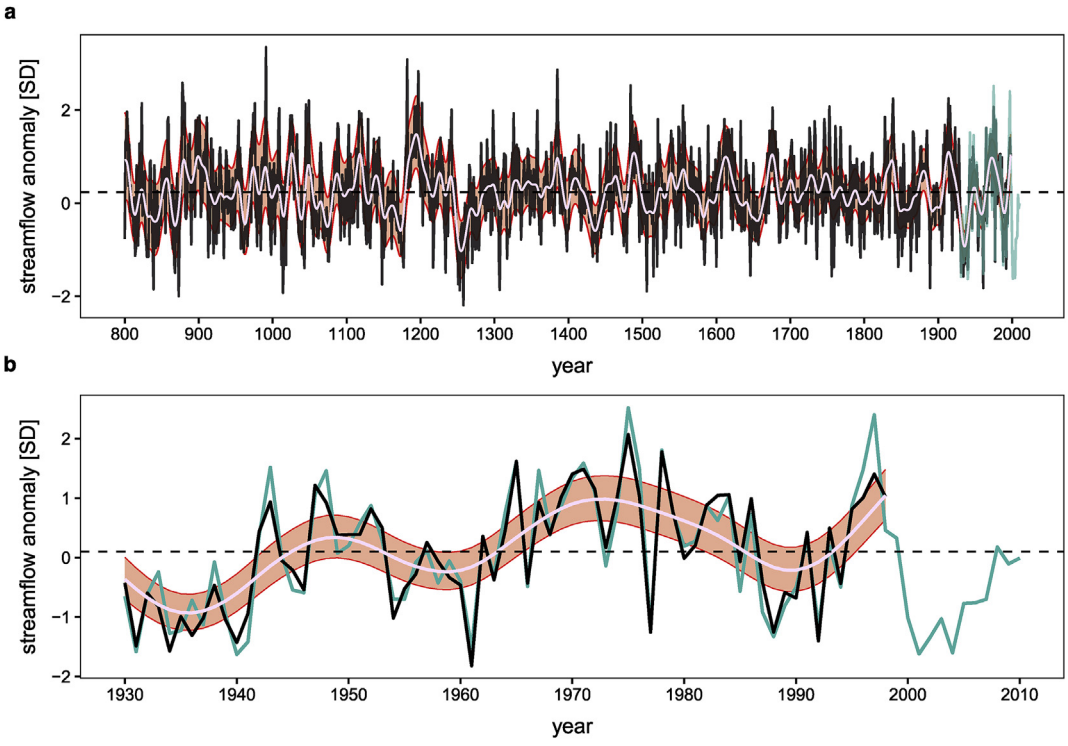

Fig. 3. **(a)** The composite streamflow reconstruction for the Upper Missouri River Basin (UMRB) (solid black line) showing a 20-year spline of reconstructed flows (white line), the correspondingly smoothed 90% confidence interval for the spline (pink ribbon), the composite observational record (blue line), and the mean of the reconstructed flows (dashed black line). **(b)** The same as (a) showing the period of the observational record. Y-axis units are standard deviations above and below the 1930–2010 observational mean. (For interpretation of the references to color in this figure legend, the reader is referred to the Web version of this article.)

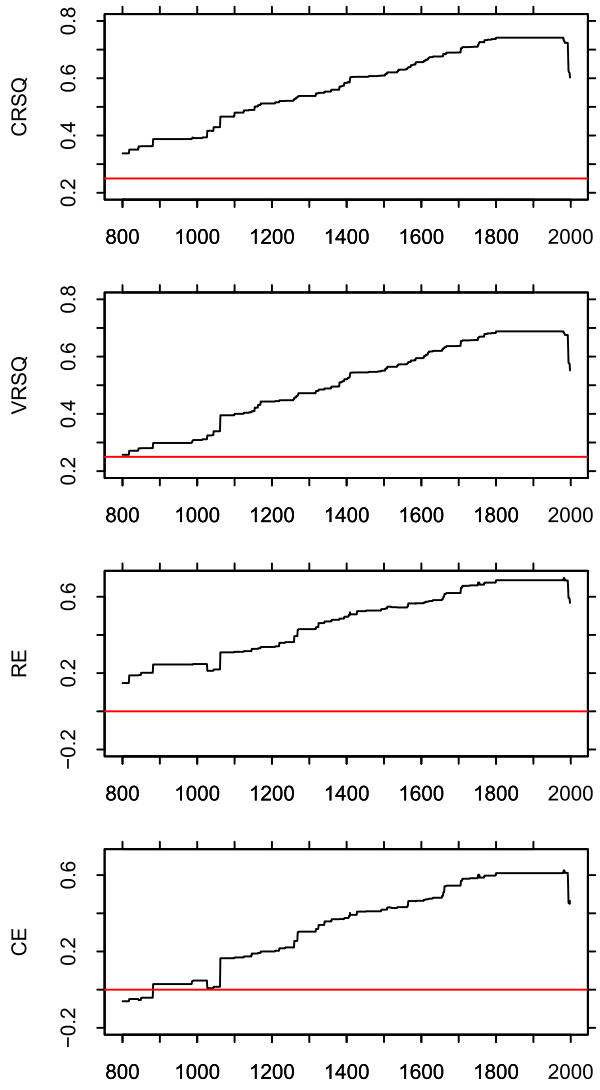

Fig. 4. Cross validation statistics for the composite streamflow record showing **(a)** the calibration coefficient of determination (R^2) (CRSQ), **(b)** verification R^2 (VRSQ), **(c)** reduction of error statistic (RE), and **(d)** coefficient of efficiency (CE).

flows for the UMRB composite correlate with those of the UCRB at Lee's Ferry such that $r = 0.44$ ($p < 0.001$ from 1930–1998 CE while for the reconstructed flows over the same period, $r = 0.43$ ($p < 0.001$). The correlation for the full reconstruction period of 800–1998 CE is very similar, ($r = 0.43$, $p < 0.001$).

In terms of sustained drought and pluvial periods, the magnitude and timing of these different phases is fairly well synchronized across the two basins (Fig. 6). Using the 60-year spline as the basis for low-frequency UMRB-UCRB agreement, wet-dry phasing is in agreement (either wet or dry in both basins) 71 percent of the time (Fig. 6) over the full record. In both basins, the period from 1100 to 1400 CE is characterized by increased persistence and amplitude in both wet and dry departures from normal flow conditions while from 1400 to 1800 CE more rapid shifts between lower amplitude wet and dry phases are generally evident.

Within the frequency domain, both similarities and differences exist between the UMRB and UCRB. In general, UMRB flow exhibits considerably more persistence than that of the UCRB with more power evident in lower-frequency modes of variability, especially during the middle part of the record (~1000–1600 CE) (Fig. 7). The MTM analysis shows that the frequency characteristics of the UMRB are relatively consistent across its sub-basins, but also highlights the considerable low-frequency power in the UMRB relative to the UCRB for periods greater than ~20 years (Fig. 8). Less power in the lower frequency signal is also evident in the Platte sub-basin which has the closest proximity to the UCRB. Conversely, the wavelet and MTM analyses also highlight considerable power in the 5–10 year periodicity for the UCRB, which is reduced greatly in both the basin-wide and sub-basin records of the UMRB (Figs. 7 and 8).

4. Discussion

4.1. Streamflow reconstructions for the UMRB and notable events in the long-term records

In this study, we present a new network of 31 tree-ring-based reconstructions of streamflow for the Upper Missouri River Basin that span nearly 1200 years and skillfully capture nearly 70% of the observed variation in the gaged records. We also present a composite record of UMRB annual streamflow anomalies built from 17 well-calibrated reconstructions for gaging locations across the five sub-regions of the UMRB. The composite record provides an important estimate of basin-wide streamflow in the Upper Missouri over the past 1200 years. This reconstruction allows, for the first time, a multi-century comparison of streamflow between the UMRB and the UCRB, two neighboring watersheds with headwaters in the US Rocky Mountains.

The most notable features of the composite record may be the exceptional pluvial event marking the turn of the 13th century, along with the equally exceptional late-12th and late 13th century drought events that bracketed this major pluvial. A similarly large magnitude and persistent dry-wet-dry swing is evident in the UCRB as well, indicating widespread synchrony in rather extreme hydroclimatic conditions across the Rockies during the Medieval period. This period of persistent, large-magnitude drought and pluvial events in the UMRB and UCRB is then followed by a comparatively quiescent period of low magnitude, short duration flow anomalies during the Little Ice Age (~1400–1900 CE).

4.2. Spatial patterns of streamflow in the UMRB and UCRB

Inter-basin temporal correlations between reconstructed streamflow records for the observed period (1930–1998) are similar to temporal correlations between observed streamflow records for this same period (Fig. 5a and b). While the nature of these relationships appears to vary over time (discussed below), the similarity of temporal correlations of inter-basin UMRB observed and reconstructed flows over the common period (1930–1998 CE) provides additional confidence that the reconstructions capture not only the temporal dynamics of streamflow in the UMRB over time, but also the general spatial structure of inter-basin streamflow variability from year-to-year. A negative relationship between streamflow in the UCRB compared with the Northern Tributaries is suggested by both observed records ($r = -0.04$, $p = 0.73$, $n = 69$ – not significant) and the full reconstructed records ($r = -0.14$, $p < 0.001$, $n = 1199$). The negative correlation of streamflow between the extreme northern and southern ends of the region is consistent with numerous observations of the North to South (N–S) anti-phasing of precipitation across the Rockies (Dettinger et al., 1998; Pederson et al., 2011; Wise, 2010b). However, the fact that this dipole-like behavior in streamflow is evident only when comparing the farthest northern and southern ends of the region likely reflects several underlying characteristics of regional hydroclimate.

First, the central latitude of the N–S cool-season precipitation

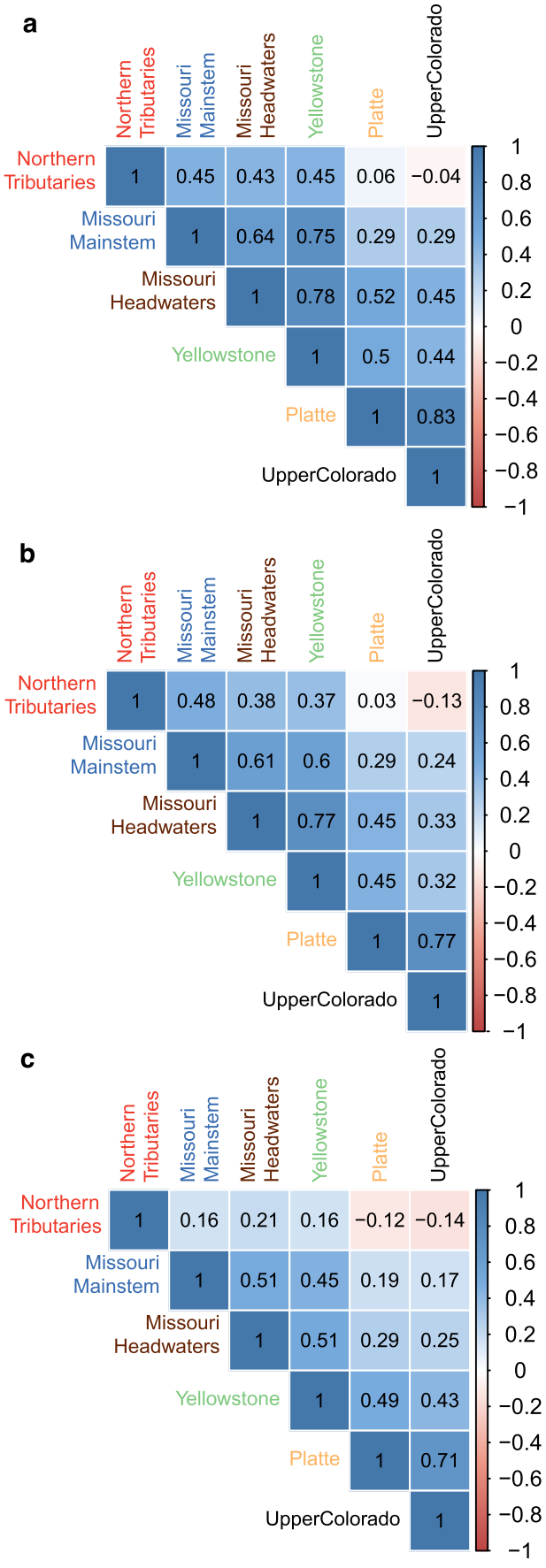

distribution over the western U.S. (*clat*) ranges primarily between 40 and 45°N over time (Dettinger et al., 1998; Wise, 2010b). However, the strength of the relationship (as expressed by temporal Pearson correlation for example) between observed precipitation anomalies and *clat* in a given year increases as one gets farther away (North or South) from this latitudinal range (Dettinger et al., 1998). Therefore, because the Northern Tributaries, as well as much of the Upper Colorado basin, lie farther from the long-term average *clat*, a N–S dipole in streamflow anomalies resulting from regional precipitation patterns is most likely to be consistently reflected in comparisons of these most northern and southern river basins.

Second, it is likely that regional temperatures play an important role in modulating the generation of streamflow from precipitation inputs across the UMRB-UCRB domain (Woodhouse et al., 2016; McCabe et al., 2017; Udall and Overpeck, 2017), and that this additional influence is expressed in broad spatial patterns that differ from those of precipitation because of differences in the underlying processes controlling spatial and temporal variability in each variable.

Finally, it is evident from the reconstructed records of streamflow that the amount of variation between sub-basins of the UMRB is not constant over time but has changed rather abruptly on several occasions over the last 1200 years. Until roughly 1400 CE, concurrent with the period of the Medieval Climate Anomaly (MCA), streamflow dynamics indicated by the 60-year spline of streamflow anomalies appear similar across all sub-basins (mean pairwise sub-basin inter-annual correlation = 0.32, $p < 0.001$) (Fig. 6). This agreement was particularly strong during the 12th and 13th centuries (mean pairwise sub-basin inter-annual correlation = 0.35, ($p < 0.001$), a period which saw the largest sustained low- and high-flow anomalies across both basins in the entire record (Fig. 6a). From ~1400 CE until ~1900 CE concurrent with the period of the Little Ice Age (LIA), inter-basin agreement was lower than during the MCA (mean pairwise sub-basin inter-annual correlation = 0.22, $p = 0.16$). Agreement then appears to increase again around 1900 CE (Fig. 6a) (mean pairwise sub-basin inter-annual correlation = 0.43, $p < 0.05$).

A consequence of decreasing agreement is a decrease in the amplitude and persistence of the basin-wide average flow record. As low flows in one portion of the basin cancel out high flows in another, the amplitude of the anomaly in the basin-wide record is decreased. Similarly, reconstructions of Pacific Decadal Variability from corals, tree rings, and historical documents have shown that the LIA was characterized by a lack of the low-frequency (pentadecadal) periodicity seen in earlier and later time periods (Biondi et al., 2001; Linsley et al., 2008; MacDonald and Case, 2005; Shen et al., 2006). The transition from the LIA into the 20th century marks the most recent shift to increased amplitude in the low-frequency dynamics of streamflow across the UMRB as well as the UCRB (Fig. 6), and corresponds to an increase in the low-frequency component of Pacific Decadal Variability (Biondi et al., 2001; Shen et al., 2006; Mccabe-Glynn et al., 2013). Given that temperature is an important variable in delineating the periods of the MCA, LIA, and 20th century, further exploration of how temperature relates to inter-basin agreement and the basin-wide amplitude of anomalies across the UMRB is warranted.

Fig. 5. Spatial correlations of (a) observed streamflow (1930–1998), (b) observational period reconstructed streamflow (1930–1998), and (c) full length reconstructed streamflow (800–1998).

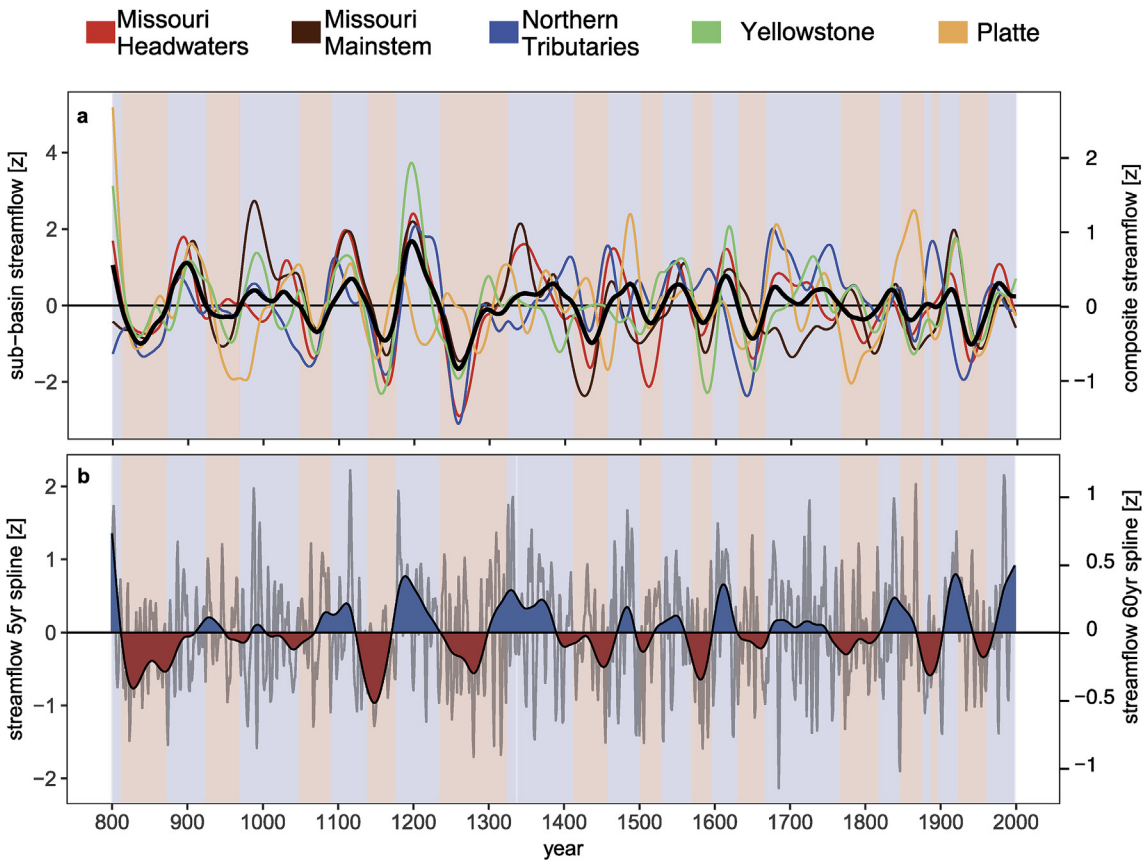

Fig. 6. 60-year splines of reconstructed streamflow for **(a)** the UMRB composite (black line) and sub-basins (colored lines) and **(b)** the UCRB. Gray lines in **b** show a 5-year spline of UCRB streamflow. Shading in both **a** & **b** indicate wet (blue) and dry (red) anomalies identified from the URMB composite 60-year spline. (For interpretation of the references to color in this figure legend, the reader is referred to the Web version of this article.)

4.3. Temporal characteristics of long-term streamflow variability in the UMRB and UCRB

In terms of basin-wide agreement between the UMRB and UCRB, several key features emerged from the 1200-year-long records of streamflow. First, the 60-year splines that characterize the multi-decadal to sub-centennial length departures from average flow are quite similar across the two basins (Fig. 6), implying that the processes controlling these gradual changes in regional hydroclimate are likely operating at a broad spatial scale over the Rocky Mountain region. As a result, persistent droughts and pluvial periods in the two basins tend to be in phase most of the time (71%). Secondly, the magnitudes of the low frequency time-series are similar over time with particularly sustained and severe wet and dry periods in both basins tracking closely through the 9th, 12th, and 13th centuries and the tendency toward shorter and less severe departures is largely mirrored on a basin-wide scale across the UMRB and UCRB during most of the LIA.

Like the UCRB (Meko et al., 2007; Woodhouse et al., 2010), the UMRB record displays multi-decadal to sub-centennial scale drought and pluvial events during the Medieval period that are significantly larger and longer than those evident over the period of the instrumental record (Fig. 6). The most sustained, and consequently largest sub-centennial scale drought in the UCRB occurred over the middle of the 12th century, although year-to-year departures were quite moderate over this period. The most severe and possibly most sustained drought in the UMRB appears during the mid-13th century and was punctuated by a severely dry decade similar to that which occurred over the region during the 1930s Dustbowl drought (Fig. 3a). Interestingly, in both the UMRB and UCRB, the wettest period on record as indicated by the 60-year spline (late 12th to mid 13th centuries) falls directly between these two driest periods (Fig. 6), suggesting a roughly 200-year epoch of unprecedented persistence and amplitude in hydroclimatic variability over the greater Rocky Mountain region during Medieval times.

The strong persistence in flow conditions characterizing this period is clearly evident in the wavelet analyses for both the UMRB and UCRB. Both basins exhibit significant power in the low-frequency streamflow signal at wavelengths of roughly 128 years (Fig. 7). While this low frequency signal is strong in the UCRB from ~1100 to 1400 CE, it is a much more dominant feature of streamflow record in the UMRB in general, where a roughly centennial-length cycle is evident throughout the entire MCA, and well in to the early portion of the LIA. In fact, it is clear from both the wavelet (Fig. 7) and MTM spectral (Fig. 8) analyses that the UMRB is generally a slower changing basin than the UCRB. The UMRB displays significant power in the multi-decadal to sub-centennial modes of variability throughout the 1200-year record and lacks the frequent tendency towards dominant inter-annual to decadal scale modes of variability evident in the UCRB.

It is important to consider that the estimation of low frequency signals in tree-ring based proxy records are affected by both inherent features of the tree-ring records themselves (Cook et al., 1995) and methodological choices made during the chronology building process (Briffa et al., 1992; Cook et al., 1990; Esper et al., 2002). Considering this we also compared the frequency characteristics of the comparable Lee's B standard chronology

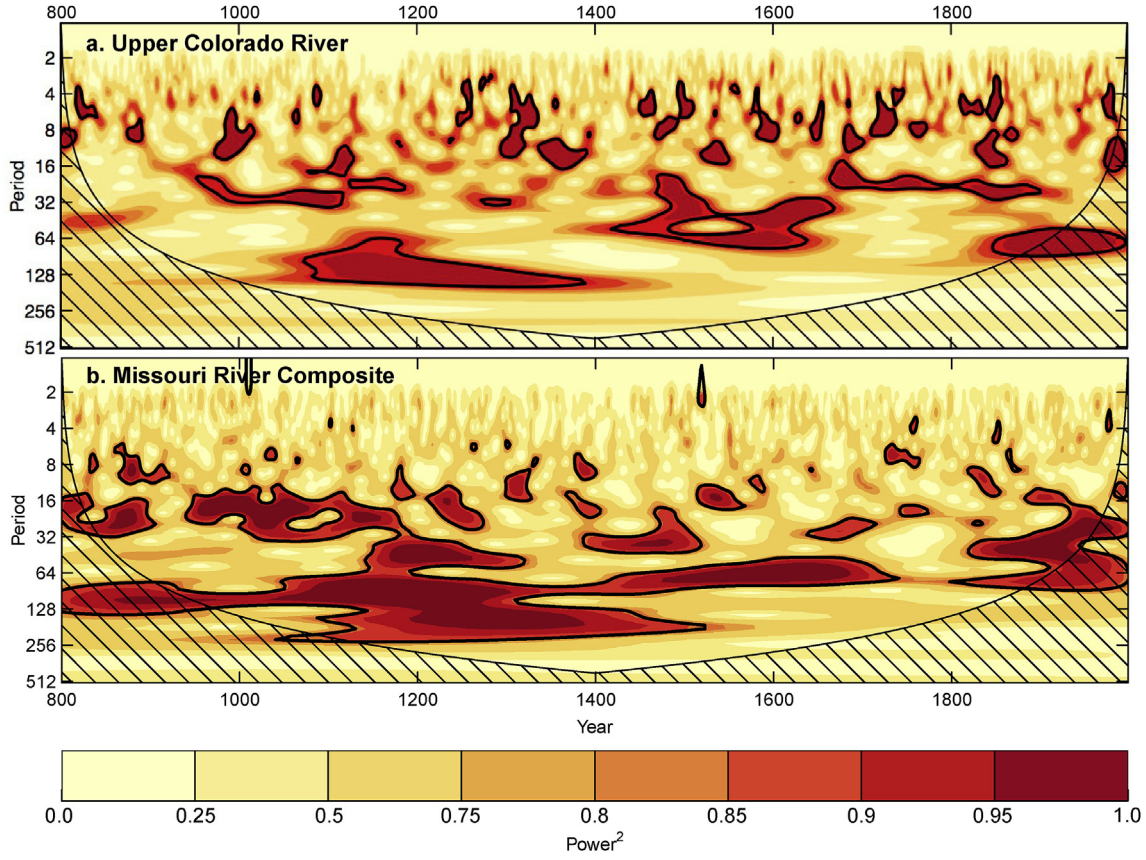

Fig. 7. Wavelet analyses for the **(a)** UCRB at Lee's Ferry and **(b)** UMRB composite time series of water-year flow. The abscissa shows time (water year) and the ordinate is modulating periodicity (period in year). Spectral power is color coded by percentage of each reconstruction spectral power distribution with levels shown on the color bar, and 95% confidence intervals are provided outlining areas of significant power exceeding that of a bootstrapped random autoregressive 1 rednoise distribution. The cross-hatched regions on either end indicate the "cone of influence," where edge effects become important. (For interpretation of the references to color in this figure legend, the reader is referred to the Web version of this article.)

reconstruction for the UCRB from Woodhouse et al. (2006) to the UMRB composite in addition to that of Meko et al. (2007) used in this study. We found that in both cases, the persistence of streamflow across the UMRB was considerably greater than that of the UCRB. To the extent that the greater reconstruction persistence of the UMRB relative to that of the UCRB accurately represents true differences in the dynamics of the basins, this finding aligns with previous work suggesting an ENSO associated, dipolar patterning of precipitation and drought that is well modulated by slow-changing climate processes such as the AMO and PDO (McCabe et al., 2004; Wise, 2010b). Because most of the UMRB lies north of the dipole transition zone of roughly 40–42°N (Wise, 2010b), persistent precipitation and drought patterns influenced by the long-term phasing of these persistent climate processes are likely to be more consistent over the UMRB than the UCRB. This is because the UCRB is approximately bisected by the dipole transition zone, meaning slow changing AMO/PDO influences on streamflow manifested in dipolar weather patterning may be more mixed, and as a result, weaker across the UCRB.

5. Conclusion

We have reconstructed streamflow for a network of gages across the UMRB back to the early 800s using an updated network of climate-sensitive tree-ring chronologies. The reconstructions are currently being used to provide a long-term perspective on variability in UMRB water supplies, as well as for providing estimates of moisture regime shift probabilities across the western U.S. (Gangopadhyay et al., 2019) and historical drought and pluvial frequencies and durations across the basin to support various planning studies by the U.S. Bureau of Reclamation and partners. In addition, these reconstructions have enabled the first long-term estimate of hydrologic variability across the entire UMRB and an assessment of how individual sub-basins have contributed to that variability over time.

In comparing the 1200-year record of streamflow in the UMRB to that of the UCRB it is evident that high-magnitude and long-duration streamflow anomalies not represented in the observed record were widespread across the Rocky Mountain region during the Medieval period, with the most severe drought and pluvial events in both basins occurring in quick succession over the 12th and 13th centuries. The Little Ice Age emerged as a period of increased spatial variability in streamflow between sub-basins within the UMRB. Basin-wide annual streamflow anomalies in both the UMRB and UCRB are moderately correlated over the full length of the record; however, the low frequency dynamics that define prolonged wet and dry departures from average flow conditions are very similar over time. As such, persistent wet and dry periods affecting the UCRB are frequently mirrored in the UMRB, affecting water supplies and challenging flood control operations for a large portion of the country.

Finally, the network of reconstructions presented here, in concert with those already available for other river basins across the West, can aid in generating key insights into the long-term nature of spatial and temporal variability of streamflow on a West-wide basis (e.g. Gangopadhyay et al., 2019). In a region heavily

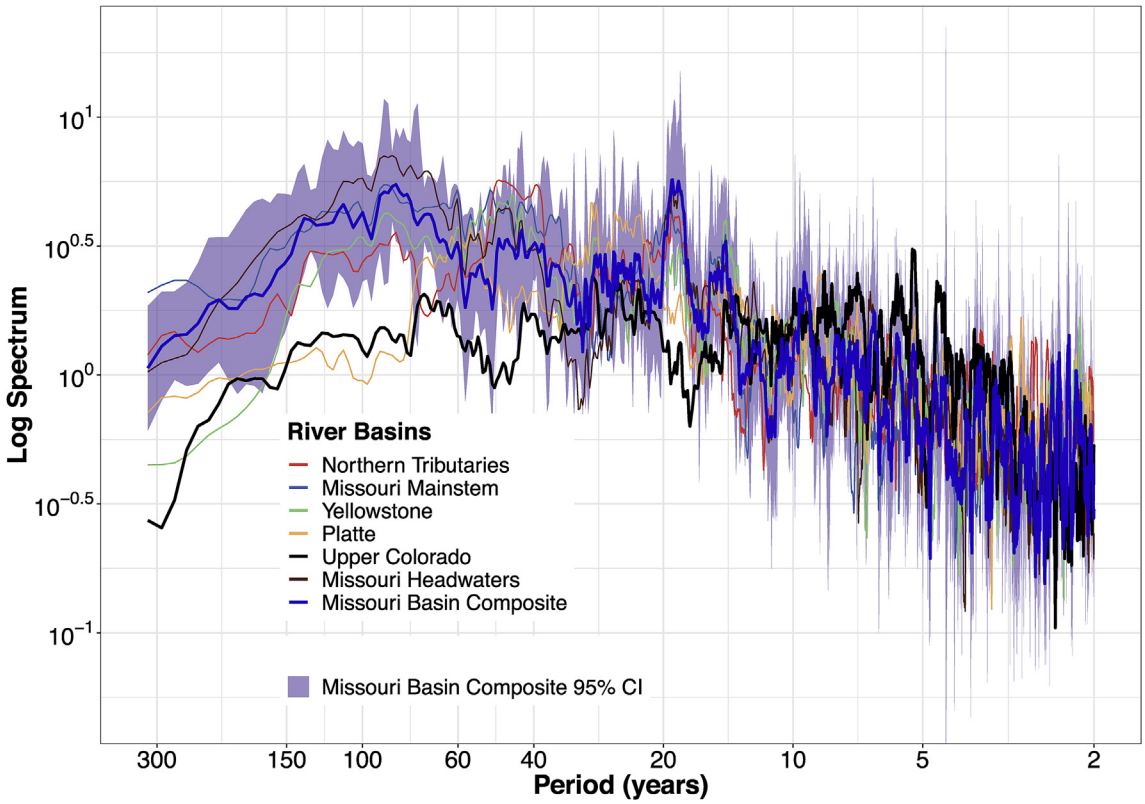

Fig. 8. The Missouri River sub-basins (colored lines), UMRB composite (heavy blue line), and UCRB at Lee's Ferry (heavy black line) streamflow reconstruction multi-taper method (MTM) spectral density estimates shown with the UMRB composite bootstrapped 95 percent (%) confidence intervals (CI) (blue shading). Axes are plotted on a $\log_{10}$ scale with frequency plotted in years (1/frequency) to aide interpretation. (For interpretation of the references to color in this figure legend, the reader is referred to the Web version of this article.)

dependent on surface water supplies, already struggling to meet increasing water demands in dry years, and facing an uncertain hydrologic outlook due to recent observed changes in temperature and snowpack development (Mote et al., 2018; Portmann et al., 2009), a spatially broad, long-term perspective of streamflow provides an important baseline understanding of hydrologic variability with which to contextualize current and future conditions on the region's rivers.

Data availability

The naturalized streamflow records used in this study as well as the reconstruction for each record are available online from the USGS (https://doi.org/10.5066/P9FC7ILX). The detrended chronologies used in the reconstruction framework are available online from the USGS (https://doi.org/10.5066/P9FC7ILX). The full set of individual raw tree-ring-width records are now available on the International Tree-Ring Data Bank (ITRDB) hosted by the National Oceanic and Atmospheric Administration (NOAA) National Climatic and Data Center (NCDC) at https://www.ncdc.noaa.gov/paleo-search/study/26831.

Acknowledgements

Research support provided through the National Science Foundation (NSF) Paleo Perspectives on Climate Change (P2C2) Program (Grant No. 1404188, 1403957, and 1401549), the NSF Graduate Research Fellowship Program (GRFP; Grant No. 1049562) and the Graduate Research Internship Program (GRIP), the U.S. Bureau of Reclamation WaterSMART Program (Sustain and Manage America's Resources for Tomorrow), the state of Montana Department of Natural Resources and Conservation, and the U.S. Geological Survey Land Resources Mission Area and the North Central Climate Adaptation Science Center. Any findings and conclusions or recommendations expressed in this material are those of the author(s) and do not necessarily reflect the views of the National Science Foundation or any official agency but do reflect the views of the U.S. Geological Survey. Coordination of GRIP at USGS is through the Youth and Education in Science programs within the Office of Science Quality and Integrity. Any use of trade, firm, or product names is for descriptive purposes only and does not imply endorsement by the U.S. Government. Lamont-Doherty Earth Observatory contribution number 8356.

Appendix A. Supplementary data

Supplementary data to this article can be found online at https://doi.org/10.1016/j.quascirev.2019.105971.

References

Biondi, F., Gershunov, A., Cayan, D.R., 2001. North Pacific decadal climate variability since 1661. J. Clim. 14, 5–10. https://doi.org/10.1175/1520-0442(2001)014%3c0005:NPDCVS%3e2.0.CO;2.

Box, G., Cox, D., 1964. An analysis of transformations. J. R. Stat. Soc. B26, 211–246.

Brekke, L.D., Kiang, J.E., Olsen, J.R., Pulwarty, R.S., Raff, D.A., Turnipseed, D.P., Webb, R.S., White, K.D., 2010. Climate change and water resources management—a federal perspective. U. S. Geol. Surv. Circ. 1331.

Briffa, K.R., Jones, P.D., Bartholin, T.S., Eckstein, D., Schweingruber, F.H., Karlen, W., Zetterberg, P., Eronen, M., 1992. Fennoscandian summers from AD 500: temperature changes on short and long timescales. Clim. Dyn. 7, 111–119.

Briffa, K.R., Jones, P.D., Pilcher, J.R., Hughes, M.K., 1988. Reconstructing summer temperatures in northern Fennoscandinavia back to A.D. 1700 using tree-ring

data from Scots pine. Arct. Alp. Res. 20, 385–384.
Cary, L.E., Parrett, C., 1996. Synthesis of Natural Flows at Selected Sites in the Upper Missouri River Basin, Montana, 1928-89, Montana. USGS Water-Resources Investigations. Report 95-4261.
Chase, K.J., 2014. Streamflow Statistics for Unregulated and Regulated Conditions for Selected Locations on the Upper Yellowstone and Bighorn Rivers, Montana and Wyoming, 1928–2002. USGS Scientific Investigations Rep, pp. 2014–5115.
Christensen, N.S., Lettenmaier, D.P., 2006. A multimodel ensemble approach to assessment of climate change impacts on the hydrology and water resources of the Colorado River Basin. Hydrol. Earth Syst. Sci. 3, 3727–3770. https://doi.org/10.5194/hess-11-1417-2007.
Cook, E.R., Briffa, K.R., Meko, D.M., Graybill, D.A., Funkhouser, G., 1995. The "segment length curse" in long tree-ring chronology development for palaeoclimatic studies. Holocene 5, 229–237.
Cook, E.R., Briffa, K.R., Shiyatov, S.G., Mazepa, V.S., 1990. Tree-ring standardization and growth-trend estimation. In: Cook, Edward R., Kairiukstis, L.A. (Eds.), Methods of Dendrochronology, Applications in the Environmental Sciences. Springer, New York, pp. 104–123.
Cook, E.R., Kairiukstis, L.A., 1990. Methods of Dendrochronology: Applications in the Environmental Sciences. Kluwer Academic Publishers, Boston.
Cook, E.R., Krusic, P.J., Melvin, T.M., 2016. RCS Signal-free Batch Processing Program. Version 47(b).
Cook, E.R., Seager, R., Heim, R.R.J., Vose, R.S., Herweijer, C., Woodhouse, C., 2010. Megadroughts in North America: placing IPCC projections of hydroclimatic change in a long-term paleoclimate context. J. Quat. Sci. 25, 48–61.
Cook, E.R., Woodhouse, C.A., Eakin, M., Meko, D.M., Stahle, D.W., 2004. Long-term aridity changes in the western United States. Science (80-.) 306, 1015–1018. https://doi.org/10.1126/science.1102586.
Daly, C., Halbleib, M., Smith, J.I., Gibson, W.P., Dogget, M.K., Taylor, G.H., Curtis, J., Pasteris, P.P., 2008. Physiographically sensitive mapping of climatological temperature and precipitation across the conterminous United States. Int. J. Climatol. 28, 2031–2064.
Dettinger, M.D., Cayan, D.R., Diaz, H.F., Meko, D.M., 1998. North-South precipitation patterns in western North America on interannual-to-decadal timescales. J. Clim. 11, 3095–3111. https://doi.org/10.1175/1520-0442(1998)011%3c3095:NSPPIW%3e2.0.CO;2.
Dettinger, M.D., Cayan, D.R., Meyer, M.K., Jeton, A., 2004. Simulated hydrologic responses to climate variations and change in the Merced, Carson, and American River basins, Sierra Nevada, California, 1900-2099 *. Clim. Change 62, 283–317. https://doi.org/10.1023/B:CLIM.0000013683.13346.4f.
Dorfman, R., 1938. A note on the delta method for finding variance formulae. Biom. Bull. 1, 129–137.
Earle, C.J., Fritts, H.C., 1986. Reconstructing Riverflow in the Sacramento River Basin since 1560. California Department of Water Resources Report DWR. B-55395.
Enfield, D.B., Mestas-Nunez, A.M., Trimble, P.J., 2001. The Atlantic multidecadal oscillation and its relation to rainfall and river flows in the continental. U.S. Geophys. Res. Lett. 28, 2077–2080.
Esper, J., Cook, E.R., Schweingruber, F.H., 2002. Low-frequency signals in long tree-ring chronologies for reconstructing past temperature variability. Science (80-.) 295, 2250–2253. https://doi.org/10.1126/science.1066208.
Falcone, J., 2011. GAGES-II: Geospatial Attributes of Gages for Evaluating Streamflow.
Fritts, H.C., 1976. Tree Rings and Climate. Academic, San Diego.
Gangopadhyay, S., Mccabe, G., Pederson, G., Martin, J., Littell, J.S., 2019. Risks of hydroclimatic regime shifts across the western United States. Sci. Rep. 9, 6303. https://doi.org/10.1038/s41598-019-42692-y.
Gangopadhyay, S., Pruitt, T., 2010. Climate Change Analysis for the St . Mary and Milk River Systems in Montana. Reclamation Technical Memorandum No. 86-68210–2010-04.
Garrick, D., Jacobs, K., Garfin, G.M., 2008. Decision making under uncertainty: shortage, stakeholders and modeling in the Colorado River basin. J. Am. Water Resour. Assoc. 44, 381–398.
Graumlich, L.J., Pisaric, M.F., Waggoner, L.A., Littell, J.S., King, J.C., 2003. Upper Yellowstone river flow and teleconnections with Pacific basin climate variability during the past three centuries article. Clim. Change 59, 245–262. https://doi.org/10.1023/A.
Gray, S.T., Graumlich, L.J., Betancourt, J.L., 2007. Annual precipitation in the Yellowstone national Park region since AD 1173. Quat. Res. 68, 18–27. https://doi.org/10.1016/j.yqres.2007.02.002.
Hamlet, A.F., Lettenmaier, D.P., 1999. Effects of climate change on hydrology and water resources in the Columbia River Basin. J. Am. Water Resour. Assoc. 35, 1597–1623.
Hidalgo, H.G., Dracup, J.A., 2003. ENSO and PDO effects on hydroclimatic variations of the Upper Colorado River Basin. J. Hydrometeorol. 4, 5–23.
Hidalgo, H.G., Piechota, T.C., Dracup, J.A., 2000. Alternative principal components regression procedures for dendrohydrologic reconstructions. Water Resour. Res. 36, 3241–3249. https://doi.org/10.1029/2000WR900097.
Ho, M., Lall, U., Cook, E.R., 2016. Can a paleodrought record be used to reconstruct streamflow?: a case study for the Missouri River Basin. Water Resour. Res. 52, 5195–5212. https://doi.org/10.1002/2015WR018444.Received.
Lehner, F., Wood, A.W., Llewellyn, D., Blatchford, D.B., Goodbody, A.G., Pappenberger, F., 2017. Mitigating the impacts of climate nonstationarity on seasonal streamflow Predictability in the U.S. Southwest. Geophys. Res. Lett. 44, 12,208–12,217. https://doi.org/10.1002/2017GL076043.
Lettenmaier, D.P., Gan, T.Y., 1990. Hydrologic sensitivities of the Sacramento-San Joaquin, California, to global warming. Water Resour. Res. 26, 69–86.
Linsley, B.K., Zhang, P., Kaplan, A., Howe, S.S., Wellington, G.M., 2008. Interdecadal-decadal climate variability from multicoral oxygen isotope records in the South Pacific Convergence Zone region since 1650 A.D. Paleoceanography 23, PA2219. https://doi.org/10.1029/2007PA001539.
Littell, J.S., Pederson, G.T., Gray, S.T., Tjoelker, M., Hamlet, A.F., Woodhouse, C.A., 2016. Reconstructions of Columbia River streamflow from tree-ring chronologies in the Pacific northwest, USA. J. Am. Water Resour. Assoc. 52, 1121–1141. https://doi.org/10.1111/1752-1688.12442.
Livneh, B., Hoerling, M.P., Badger, A.M., Eischeid, J.K., Webb, R.S., 2016. Causes for hydrologic extremes in the upper Missouri river basin. In: NOAA Climate Assessment Report.
Lumley, A.T., Miller, A., 2004. The Leaps Package.
Lutz, E.R., Hamlet, A.F., Littell, J.S., 2012. Paleoreconstruction of cool season precipitation and warm season streamflow in the Pacific Northwest with applications to climate change assessments. Water Resour. Res. 48, W01525. https://doi.org/10.1029/2011WR010687.
MacDonald, G.M., Case, R.A., 2005. Variations in the Pacific decadal oscillation over the past millennium. Geophys. Res. Lett. 32, L08703. https://doi.org/10.1029/2005GL022478.
Mallows, C.L., 1973. Some comments on Cp. Technometrics 15, 661–675.
Mann, M.E., Lees, J., 1996. Robust estimation of background noise and signal detection in climatic time series. Clim. Change 33, 409–445. https://doi.org/10.1007/BF00142586.
McCabe, G.J., Palecki, M.A., Betancourt, J.L., 2004. Pacific and Atlantic Ocean influences on multidecadal drought frequency in the United States. Proc. Natl. Acad. Sci. 101, 4136–4141. https://doi.org/10.1073/pnas.0306738101.
McCabe, G.J., Wolock, D.M., 2011a. Independent effects of temperature and precipitation on modeled runoff in the conterminous United States. Water Resour. Res. 47, W11522. https://doi.org/10.1029/2011WR010630.
McCabe, G.J., Wolock, D.M., 2011b. Century-scale variability in global annual runoff examined using a water balance model. Int. J. Climatol. 31, 1739–1748. https://doi.org/10.1002/joc.2198.
McCabe, G.J., Wolock, D.M., Pederson, G.T., Woodhouse, C.A., McAfee, S., 2017. Evidence that recent warming is reducing upper Colorado river flows. Earth Interact. 21. https://doi.org/10.1175/EI-D-17-0007.1.
Mccabe-Glynn, S., Johnson, K.R., Strong, C., Berkelhammer, M., Sinha, A., Cheng, H., Edwards, R.L., 2013. Variable North Pacific influence on drought in southwestern North America since AD 854. Nat. Geosci. 6, 617–621. https://doi.org/10.1038/ngeo1862.
McCarroll, D., Young, G.H.F., Loader, N.J., 2015. Measuring the skill of variance-scaled climate reconstructions and a test for the capture of extremes. Holocene 25, 618–626. https://doi.org/10.1177/0959683614565956.
Meko, D.M., Woodhouse, C.A., Baisan, C.A., Knight, T., Lucas, J.J., Hughes, M.K., Salzer, M.W., 2007. Medieval drought in the upper Colorado river basin. Geophys. Res. Lett. 34, 1–5. https://doi.org/10.1029/2007GL029988.
Melvin, T.M., Briffa, K.R., 2008. A "signal-free" approach to dendroclimatic standardisation. Dendrochronologia 26, 71–86. https://doi.org/10.1016/j.dendro.2007.12.001.
Melvin, T.M., Brifffa, K.R., Nicolussi, K., Grabner, M., 2007. Time-varying-response smoothing. Dendrochronologia 25, 65–69. https://doi.org/10.1016/j.dendro.2007.01.004.
Mote, P.W., Li, S., Lettenmaier, D.P., Xiao, M., Engel, R., 2018. Dramatic declines in snowpack in the western US. Clim. Atmos. Sci. 1, 2. https://doi.org/10.1038/s41612-018-0012-1.
Murtagh, F., 1985. Multidimensional clustering algorithms. In: COMPSTAT Lectures 4. Physica-Verlag, Wuerzburg.
Norton, P.A., Anderson, M.T., Stamm, J.F., 2014. Trends in Annual, Seasonal, and Monthly Streamflow Characteristics at 227 Streamgages in the Missouri River Watershed, Water Years 1960 – 2011 Scientific Investigations Report 2014 – 5053 128. https://doi.org/10.3133/sir2014505.
Nowak, K., Hoerling, M., Rajagopalan, B., Zagona, E., 2012. Colorado river basin hydroclimatic variability. J. Clim. 25, 4389–4403. https://doi.org/10.1175/JCLI-D-11-00406.1.
Pederson, G.T., Gray, S.T., Woodhouse, C.A., Betancourt, J.L., Fagre, D.B., Littell, J.S., Watson, E., Luckman, B.H., Graumlich, L.J., 2011. The unusual nature of recent snowpack declines in the north American Cordillera. Science (80-.) 333, 332–336.
Pendergrass, A.G., Knutti, R., Lehner, F., Deser, C., Sanderson, B.M., 2017. Precipitation variability increases in a warmer climate. Sci. Rep. 7, 1–9. https://doi.org/10.1038/s41598-017-17966-y.
Portmann, R.W., Solomon, S., Hegerl, G.C., 2009. Spatial and seasonal patterns in climate change, temperatures, and precipitation across the United States. Proc. Natl. Acad. Sci. 106, 7324–7329. https://doi.org/10.1073/pnas.0808533106.
Prairie, J., Nowak, K., Rajagopalan, B., Lall, U., Fulp, T., 2008. A stochastic nonparametric approach for streamflow generation combining observational and paleoreconstructed data. Water Resour. Res. 44, W06423. https://doi.org/10.1029/2007WR006684.
Redmond, K.T., Koch, R.W., 1991. Surface climate and streamflow variability in the western United States and their relationship to large-scale circulation indices. Water Resour. Res. 27, 2381–2399.
Seaber, P.R., Kapinos, F., Knapp, G.L., 1987. Hydrologic Unit Maps - Water Supply Paper 2294.
Shen, C., Wang, W.C., Gong, W., Hao, Z., 2006. A Pacific Decadal Oscillation record since 1470 AD reconstructed from proxy data of summer rainfall over eastern

China. Geophys. Res. Lett. 33, L03702. https://doi.org/10.1029/2005GL024804.
Slack, J.R., Lumb, A.M., Landwehr, J.M., 1994. Hydro-Climatic Data Network (HCDN) - A USGS Streamflow Data Set for the U.S. For the Study of Climate Fluctuations.
George, S. St., 2014. An overview of tree-ring width records across the Northern Hemisphere. Quat. Sci. Rev. 95, 132–150. https://doi.org/10.1016/j.quascirev.2014.04.029.
Stewart, I.T., Cayan, D.R., Dettinger, M.D., 2005. Changes toward earlier streamflow timing across western North America. J. Clim. 18, 1136–1155. https://doi.org/10.1175/JCLI3321.1.
Stockton, C.W., Jacoby, G.C., 1976. Long-term surface-water supply and streamflow trends in the Upper Colorado River Basin. Lake Powell Res. Proj. Bull. 18. Natl. Sci. Found., Arlington, Va.
Torrence, C., Compo, G.P., 1998. A Practical guide to wavelet analysis. Bull. Am. Meteorol. Soc. 79, 61–78.
U.S. Department of Agriculture, 1994. State Soil Geographic (STATSGO) Data Base: Data Use Information. USDA Miscellaneous Publ. 1492, p. 113.
Udall, B., Overpeck, J., 2017. The twenty-first century Colorado River hot drought and implications for the future. Water Resour. Res. 53, 2404–2418. https://doi.org/10.1002/2016WR019638.Received.
Watson, T.A., Anthony Barnett, F., Gray, S.T., Tootle, G.A., 2009. Reconstructed streamflows for the headwaters of the Wind river, Wyoming, United States. J. Am. Water Resour. Assoc. 45, 224–236. https://doi.org/10.1111/j.1752-1688.2008.00274.x.
Wettstein, J.J., Littell, J.S., Wallace, J.M., Gedalof, Z., 2011. Coherent region-, species-, and frequency-dependent local climate signals in northern hemisphere tree-ring widths. J. Clim. 24, 5998–6012. https://doi.org/10.1175/2011JCLI3822.1.
Wise, E.K., 2010a. Tree ring record of streamflow and drought in the upper Snake River. Water Resour. Res. 46, W11529. https://doi.org/10.1029/2010WR009282.
Wise, E.K., 2010b. Spatiotemporal variability of the precipitation dipole transition zone in the western United States. Geophys. Res. Lett. 37, L07706. https://doi.org/10.1029/2009GL042193.
Wise, E.K., Woodhouse, C.A., McCabe, G.J., Pederson, G.T., St-Jacques, J.M., 2018. Hydroclimatology of the Missouri river basin. J. Hydrometeorol. 19, 161–182. https://doi.org/10.1175/JHM-D-17-0155.1.
Woodhouse, C.A., 2001. A tree-ring reconstruction of streamflow for the Colorado Front Range. J. Am. Water Resour. Assoc. 37, 561–569.
Woodhouse, C.A., Gray, S.T., Meko, D.M., 2006. Updated streamflow reconstructions for the upper Colorado river basin. Water Resour. Res. 42, W05415. https://doi.org/10.1029/2005WR004455.
Woodhouse, C.A., Lukas, J.J., Morino, K., Meko, D.M., Hirschboeck, K.K., 2017. Using the past to plan for the future-the value of paleoclimate reconstructions for water resource planning. In: Miller, K.A., Hamlet, A.F., Kenney, D.S., Redmond, K.T. (Eds.), Water Policy and Planning in a Variable and Changing Climate. CRC Press, Boca Raton, FL, pp. 161–182. https://doi.org/10.1201/b19534.
Woodhouse, C.A., Meko, D.M., MacDonald, G.M., Stahle, D.W., Cook, E.R., 2010. A 1,200-year perspective of 21st century drought in southwestern North America. Proc. Natl. Acad. Sci. 107, 21283–21288. https://doi.org/10.1073/pnas.0911197107.
Woodhouse, C.A., Pederson, G.T., Morino, K., McAfee, S.A., McCabe, G.J., 2016. Increasing influence of air temperature on upper Colorado River streamflow. Geophys. Res. Lett. 43, 2174–2181. https://doi.org/10.1002/2015GL067613.
Yoon, J.H., Wang, S.Y.S., Gillies, R.R., Kravitz, B., Hipps, L., Rasch, P.J., 2015. Increasing water cycle extremes in California and in relation to ENSO cycle under global warming. Nat. Commun. 6, 1–6. https://doi.org/10.1038/ncomms9657.